Available online at www.sciencedirect.com
SCIENCE DIRECT®
Neuroscience Letters 370 (2004) 206–211
Neuroscience Letters
www.elsevier.com/locate/neulet

# MR perfusion-weighted imaging and quantitative analysis of cerebral hemodynamics with symptom provocation in unmedicated patients with obsessive–compulsive disorder

Xiao-Li Chen[a], Jing-Xia Xie[a], Hong-Bin Han[a,*], Yu-Hua Cui[b], Bai-Quan Zhang[b]

[a] *Department of Radiology, Third Hospital of Peking University Health Science Center, 49 North Garden Road, Haidian District, Beijing 100083, PR China*
[b] *Beijing Mental Health Collaborating Center, Peking University Health Science Center, Beijing, PR China*

Received 6 April 2004; received in revised form 23 June 2004; accepted 11 August 2004

**Abstract**

We evaluated the potential effectiveness of dynamic contrast-enhanced perfusion-weighted images (PWI) in determining hemodynamic activation in brain structures that may be involved in mediating the symptomatology of patients with obsessive–compulsive disorder (OCD), as manifested by contamination obsessions with washing compulsions. Ten unmedicated female patients with OCD were subjected to PWI, and relative cerebral blood flow (rCBF) in each region of interest (ROI) and self-ratings of OCD symptoms were compared before and after symptom provocation. We found that increases in the Anxiety Analogue Scale (AAS) and OCD Analogue Scale (OCDAS) scores were each significantly associated with provocation. The correlations between OCDAS and AAS scores were also statistically significant during both the control and provoked conditions. Compared with the control state, there was a significant increase in rCBF during the symptomatic state in the right head of caudate nucleus, thalamus, and bilateral orbitofrontal cortices (OFC). No statistical changes in rCBF were found in the bilateral anterior cingulate cortices (ACC). These findings demonstrate that OCD symptomatology is accompanied by anxiety, and that abnormal features are particularly apparent in the orbitofrontal-subcortical circuits.


*Keywords:* Perfusion-weighted imaging; Cerebral blood flow; Obsessive–compulsive disorder; Symptom provocation; Drug-free; Contamination

Obsessive–compulsive disorder (OCD) is a common psychiatric disorder. Despite dramatic advances in the pharmacologic and behavioral treatment of patients with OCD, there remains much to be learned about its pathophysiology. Three different functional imaging study designs have been used to elucidate the pathophysiology of OCD: comparing subjects with OCD with normal controls; scanning subjects with OCD before and after treatment to measure metabolic changes which correspond to treatment response; and activation studies in which patients are scanned both in the resting state and during provocation of their symptoms or during a cognitive activation task. Using functional imaging techniques, including positron emission tomography (PET), single photon emission computed tomography (SPECT), and dynamic contrast-enhanced perfusion-weighted images (PWI), a wide variety of neural dysfunctions have been implicated in the pathophysiology of obsessive–compulsive disorder (OCD). The structures involved in the prefrontal-striatal-thalamocortical circuits have often been reported as hyperactive in resting brain-imaging studies in OCD patients [15,17]. Additionally, studies performed before and after treatment [18,19] have suggested a possible role of other neuroanatomic circuits involving orbitofrontal and anterior cingulate cortices, striatum, and thalami.

Symptom provocation studies in patients with OCD have shown that the structures involved in frontal-subcortical circuits are hyperactive [5,2,11,14,16], suggesting that the orbitofrontal and anterior cingulate cortices, as well as the striatum and thalami, are involved in the pathophysiology of OCD. Previous quantitative analysis of cerebral hemodynamics with symptom provocation using SPECT and PET had

* Corresponding author. Tel.: +86 10 62385612; fax: +86 10 62017700.
*E-mail address:* hhb1630@vip.sina.com (H.-B. Han).

0304-3940/$ – see front matter © 2004 Elsevier Ireland Ltd. All rights reserved.
doi:10.1016/j.neulet.2004.08.019

found that the relative cerebral blood flow (rCBF) within the orbitofrontal cortex (OFC), anterior cingulate cortex (ACC), caudate nucleus and thalamus increased after the symptom provocation [11,16]. PWI, which provides better spatial resolution than radioimaging techniques, was first used in the present study to evaluate the potential effectiveness of this technique in determining hemodynamic activation in brain structures that may be involved in mediating the symptomatology of patients with OCD. We, therefore, acquired PWI images during both control and provoked states in unmedicated OCD patients with contamination obsessions and washing compulsions, and we quantitatively analyzed changes in cerebral hemodynamics occurring within each region of interest (ROI) during symptom provocation. It was proposed that the rCBF within some of the ROIs would increase after the symptom provocation, and the PWI would be a valuable technique in providing powerful evidence for the pathophysiology of OCD.

Our patient cohort consisted of 13 right-handed female outpatients, aged between 18 and 50 years, who had contamination obsessions with washing compulsions and met DSM-IV diagnostic criteria for OCD without current comorbid diagnoses. Other inclusion criteria included the absence of other neuropsychical disorders (e.g. schizophrenia, eating disorder, generalized anxiety disorder, major depression, and bipolar disorder), medical conditions (e.g. hypertension or diabetes), and non-use of drugs with central nervous system effects (also excluded nicotine use, alcohol use or other illicit drug use) for at least 30 days prior to the study. For each patient, one scan was performed before and one after provocation. Six PWI scans from three patients were excluded from analysis due to technical problems (two patients) and unacceptable motion artifacts (one patient). Thus, 20 scans from 10 patients were available for analysis. Excluded patients did not differ from active participants with respect to age, education or gender.

The mean ± S.D. age of the included patients was 26.44 ± 8.46 years (range, 18–45 years), with an average education of (mean ± S.D.) 11.33 ± 1.32 years (range, 10–13 years). The mean (±S.D.) course of OCD was 5.25 ± 8.28 years (range, 0.25–27 years), and the mean (±S.D.) severity of OCD, as measured by Yale–Brown Obsessive–Compulsive Scale (Y-BOCS), was 25.10 ± 8.43 (range, 13–40). Since all patients were scanned in both resting and provoked states, each served as her own control.

Written informed consent was obtained from each patient. The study protocol was approved by the Subcommittee on Human Studies of the Health Center of Peking University, Beijing.

Stimuli were designed by each patient and a psychiatrist prior to the scan to ensure that each patient's OCD symptomatology was effective and well tolerated. Symptom provocation and subsequent 10-point, self-reporting analogue scales were performed by each patient for about 5 h before formal studies to quantify the severity of each patient's anxiety according to the Anxiety Analogue Scale (AAS), and to quantify each patient's OCD symptoms according to the OCD Analogue Scale (OCDAS). These scales provide clinical measures by which to gauge the magnitude of patient responses to innocuous and provocative stimuli [16]. For both scales, a score of 10 was equated with the most severe symptoms previously experienced by the patient, while 0 was equated with the complete absence of symptoms.

After being placed in the scanner in a supine position, each patient was allowed to habituate to the environment, during which time analogue scale scores were obtained every 3 min. For each patient, innocuous and provocative stimuli were matched for sensory, motor, and cognitive components so that they differed only in meaning to patients and the affective state evoked. The aversive stimuli were tissues or rubber gloves contaminated with waste, whereas the innocuous stimuli were "clean" versions of the same objects (i.e. uncontaminated tissues or new rubber gloves) [16]. Immediately after placement of the stimulus, the patient was instructed to close her eyes and allow her thoughts to focus on the stimulus, following which the patient was asked to indicate the severity of her anxiety and OCD symptoms on the corresponding scales just before each PWI. When the scan was finished, the stimulus was removed. For each patient, two PWI scans were performed 30 h apart during the resting and the provoked state in random order. OCDAS and AAS scores were determined by averaging the scores at the beginning and the end of PWI.

PWI scans were performed on patients in the supine position using a 1.5-T MR imager (Siemens Magnetom Vision, Erlangen, Germany) with a quadrature head coil (Siemens Co., Germany). A pillow with foam padding was used to minimize patient movement in the head coil. Earplugs and headphones were provided to block background noise and to communicate with patients, respectively. Following routine T1- and T2-weighted imaging, a transverse high-resolution T1-weighted scan (repetition time (TR)/echo time (TE) 600/14 ms; 90° flip angle; 10 slices of 5-mm thickness each, 1-mm gap; 23-cm field of view (FOV)) was acquired for anatomic reference in a direction parallel to the anterior commissural-posterior commissural (AC-PC) plane. The upmost slice located 40 mm above the AC-PC line, and the lowest slice located 20 mm under the AC-PC line. Following exposure to a stimulus, dynamic contrast-enhanced PWI acquisitions were collected simultaneously in the same planes as the previous transverse high-resolution T1WI using a rapid T2*-weighted echo-planar free-induction-decay (FID) pulse sequence. After scanning had begun and four sets of baseline images had been acquired, each patient was administered an intravenous bolus of dimeglumine gadopentetate (Gd-DTPA, Magnevist, Schering, Berlin, Germany), 0.2 mmol/kg, at a flow rate of 4 mL/s over 3–5 s, using an automatic MR power injector (Spectris, SMR200, Medrad Inc., Pittsburgh, PA), followed immediately by a flush with the same volume of saline at the same rate. The parameters employed for PWI were TR/TE 1.2/42.1 ms, 90° flip angle, 128×128 matrix size, 23-cm FOV and 1 excitation, and 40 sets of 10 image

Table 1
The OCD and Anxiety Analogue Scale scores during the resting (or control) and the provocation state ($n$ = 10)

| OCD Analogue Scale (OCDAS) scores | | | | | | Anxiety Analogue Scale (AAS) scores | | | | | |
|---|---|---|---|---|---|---|---|---|---|---|---|
| Resting state | | | Provocation state | | | Resting state | | | Provocation state | | |
| Pre- | Post- | Mean | Pre- | Post- | Mean | Pre- | Post- | Mean | Pre- | Post- | Mean |
| 0 | 1 | 0.5 | 5 | 6 | 5.5 | 1 | 1 | 1.0 | 3 | 2 | 2.5 |
| 1 | 1 | 1.0 | 7 | 6 | 6.5 | 2 | 1 | 1.5 | 3 | 3 | 3.0 |
| 1 | 1 | 1.0 | 8 | 8 | 8.0 | 2 | 2 | 2.0 | 2 | 2 | 2.0 |
| 1 | 1 | 1.0 | 6 | 7 | 6.5 | 1 | 1 | 1.0 | 3 | 3 | 3.0 |
| 1 | 1 | 1.0 | 6 | 7 | 6.5 | 0 | 1 | 0.5 | 3 | 2 | 2.5 |
| 1 | 1 | 1.0 | 6 | 6 | 6.0 | 1 | 1 | 1.0 | 3 | 2 | 2.5 |
| 1 | 2 | 1.5 | 6 | 7 | 6.5 | 1 | 1 | 1.0 | 3 | 4 | 3.5 |
| 1 | 2 | 1.5 | 7 | 7 | 7.0 | 2 | 1 | 1.5 | 3 | 3 | 3.0 |
| 0 | 1 | 0.5 | 7 | 6 | 6.5 | 1 | 2 | 1.5 | 3 | 3 | 3.0 |
| 1 | 1 | 1.0 | 7 | 8 | 7.5 | 1 | 1 | 1.0 | 2 | 3 | 2.5 |

OCD, obsessive–compulsive disorder; pre-, pre-scaning; post-, post-scaning.

planes, which were the same as those used in the prior high-resolution T1WI. About 30 h later, the FID pulse sequence with the same location and extension as the first one was performed repeatedly while the patient was exposed to an individualized provocative/innocuous stimulus.

Image processing was performed using standard image analysis software available on the MR unit. Cerebral blood perfusion maps (CBPM) were created and analyzed. The signal intensity (SI) of ROI was measured bilaterally before and after stimulus. Changes of SI occurring during cerebral transit of the high magnetic susceptibility Gd-DTPA were converted to contrast agent concentration–time curves. The fact that the two concentration–time curves of cerebellum during the resting and the provoked state obtained in our study almost overlapped supported the cerebellum was less affected than other regions during provocations in OCD patients [16]. So we used the cerebellum as a reference region, and rCBF of each ROI (i.e. the ratios of index regional mean value to cerebellum mean value) were then calculated and analysed. Blood vessels, which appear very bright in dynamic susceptibility contrast MRI, were segmented and excluded from all regional analyses. There were four ROI measurements in each hemisphere, yielding eight ROIs including the bilateral OFC, ACC, heads of caudate nuclei, and thalami. OFC measurement was placed in supracellar cistern plane, this ROI located between orbital gyrus and inferior frontal gyrus; ACC measurement was placed in the plane displaying body of caudate nucleus, corresponding ROI located around cingulate sulcus; the rCBF values in the heads of caudate nuclei and the thalami were measured in the plane showing column of fornix. ROIs were drawn first on the right hemisphere, and mirrored ROIs were subsequently placed on the left hemisphere. Four circular regions with same size of 0.1 $cm^2$ were delineated within each ROI, and SI was measured in different regions to obtain the mean rCBF of corresponding ROI.

All statistical analyses were performed using the Statistical Package for the Social Sciences (SPSS for WINDOWS software). For all contrasts, a two-tailed statistical significance level was set at $P < 0.05$. The paired Student's $t$-test was used to compare differences in AAS and OCDAS scores between the two conditions. Pearson product–moment statistics were performed for correlations between OCDAS and AAS scores in both states. Measurements of rCBF during the two states were compared using paired Student's $t$-test.

OCDAS and AAS scores immediately before and after the control or provoked scans shown separately in Table 1 demonstrated that the stimuli persisted through the scans. The provocative stimuli designed individually for each patient included in the analyses resulted in increased OCDAS and AAS scores when compared with the scores after innocuous stimuli (Table 2). Mean (±S.D.) OCDAS scores were $1.00 \pm 0.33$ for the baseline condition and $6.65 \pm 0.71$ for the provoked condition, a statistically significant increase ($P < 0.01$). Mean AAS scores were $1.20 \pm 0.42$ for the resting condition and $2.75 \pm 0.42$ for the provoked condition, a difference that was also statistically significant ($P < 0.01$). The correlations between OCDAS and AAS scores were statistically significant for both the control ($r = 0.79$, $P = 0.006$) and provoked ($r = 0.69$, $P = 0.027$) conditions. Statistically significant increases in rCBF during the OCD symptomatic state compared with

Table 2
Comparison of the OCD and Anxiety Analogue Scale scores between resting (or control) and provocation state ($n$ = 10)

| OCD Analogue Scale (OCDAS) scores | | | | | Anxiety Analogue Scale (AAS) scores | | | | |
|---|---|---|---|---|---|---|---|---|---|
| Rest | Provocation | $t$ | d.f. | $P$ | Rest | Provocation | $t$ | d.f. | $P$ |
| $1.00 \pm 0.33$ | $1.65 \pm 0.71$[a] | −26.717 | 9 | 0.000 | $1.20 \pm 0.42$ | $2.75 \pm 0.42$[a] | −7.619 | 9 | 0.000 |

OCD, obsessive–compulsive disorder.
[a] Significantly increased after symptom provocation: paired Student's $t$-test, at the 0.05 level (two-tailed).

Table 3
Significant increase in rCBF within several ROIs after symptom prococation ($n$ = 10)

| ROIs | rCBF (ROI/cerebellar CBF ratio) (mean ± S.D.) | | $t$ | d.f. | $P$ |
|---|---|---|---|---|---|
| | Before provocation | After provocation | | | |
| Right anterior cingulate cortex | 0.61 ± 0.16 | 0.76 ± 0.12 | −0.817 | 9 | 0.438 |
| Left anterior cingulate cortex | 0.87 ± 0.15 | 1.00 ± 0.16 | −0.587 | 9 | 0.573 |
| Right orbitofrontal cortex | 1.05 ± 0.16 | 1.47 ± 0.26[a] | −2.361 | 9 | 0.043 |
| Left orbitofrontal cortex | 0.87 ± 0.10 | 1.18 ± 0.15[a] | −2.389 | 9 | 0.041 |
| Right head of caudate nucleus | 1.06 ± 0.13 | 1.38 ± 0.14[a] | −2.666 | 9 | 0.026 |
| Left head of caudate nucleus | 1.19 ± 0.20 | 1.18 ± 0.23 | 0.085 | 9 | 0.934 |
| Right thalamus | 0.79 ± 0.11 | 1.03 ± 0.16[a] | −2.527 | 9 | 0.035 |
| Left thalamus | 1.14 ± 0.24 | 1.32 ± 0.39 | −2.111 | 9 | 0.064 |

OCD, obsessive–compulsive disorder; ROI, the region of interest; CBF, the cerebral blood flow; rCBF, the relative cerebral blood flow.
[a] Significantly different from those before symptom provocation: paired Student's $t$-test, at the 0.05 level (two-tailed).

the control state were observed in the bilateral OFC, the right head of caudate nucleus, and the right thalamus (Table 3).

Our finding, that OCDAS and AAS scores were significantly increased following provocation, suggests that OCD symptoms were successfully induced during the second PWI scan. The correlation between these two scores in both the resting and provoked states provides evidence that OCD symptomatology is accompanied by anxiety in patients with OCD. The brain regions we found to be activated upon symptom provocation are mostly consistent with previous structural, neuropsychological and functional studies, suggesting that dysfunction in the OFC [1,2,5,8,13,16,20,21], striatum [5,16] and thalamus [3,4,6,14,15,19] may play a role in OCD symptomatology.

The asymmetries observed during rCBF changes in OCD partly reflect the asymmetric vasculature in the brain and the underlying asymmetry of brain function [7]. The OFC, particularly on the right side, has been found to be activated by the provocation of obsessive–compulsive symptoms [5,14,16], a finding confirmed by the results of this study. Although less consistent, abnormalities in thalamic areas have been reported across different cultures. The major function of the thalamus consists of the integration and relay of sensory and motor information. Neuropsychological studies also support the involvement of the thalamus in the pathophysiology of OCD [10].

Based on our findings and the previous neuropsychological studies, we have demonstrated a conceptual diagram of the cortical-subcortical circuitry (Fig. 1) operational during symptom mediation in OCD patients with contamination obsession and washing compulsion. The orbitofrontal-subcortical circuit originates in the OFC, which projects to striatum. The 'direct' pathway leading from striatum projects to the globus pallidus interna/substantia nigra, pars reticulata (Gpi/SNr) complex (the main output station of the basal ganglia), then to the thalamus, and back to the cortical site of origin. This pathway contains two excitatory and two inhibitory projections, making it a net 'positive feedback' loop. The 'indirect' pathway also originates in the frontal cortex and projects to the striatum, but then projects to the globus pallidus external (GPe), then to the subthalamic nucleus, frontal cortex. This indirect circuit has three inhibitory connections, making it a net 'negative feedback' loop. The imbalance of direct > indirect pathway 'tone' is regarded as the pathophysiological model of OCD. OCD symptomatology may be the result of a 'captured' signal in the direct cortical-subcortical pathway. This captured signal may be due to an imbalance between direct and indirect pathway tone, with the direct pathway having greater influence than the indirect pathway, with greater inhibition of the GPi, leading to greater thalamocortical activation.

High-speed EPI-PWI techniques are more sensitive to changes in CBF than PET or SPECT, which have the disadvantages of limited spatial and temporal resolution as well

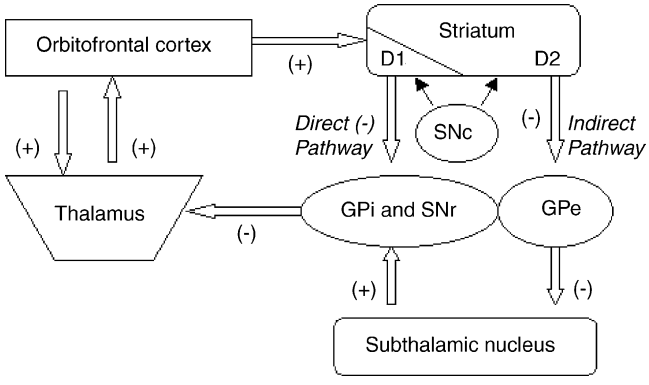


Fig. 1. A pathophysiological model of OCD speculated through the current study in patients with OCD who had contamination obsessions and washing compulsions. The orbitofrontal-subcortical circuit originates in the orbitofrontal cortices (OFC), which projects to striatum. The 'direct' pathway leading from striatum projects to the Gpi/SNr complex (the main output station of the basal ganglia), then to the thalamus, and back to the cortical site of origin. This pathway contains two excitatory and two inhibitory projections, making it a net 'positive feedback' loop. The 'indirect' pathway also originates in the frontal cortex and projects to the striatum, but then projects to the GPe, then to the subthalamic nucleus, frontal cortex. This indirect circuit has three inhibitory connections, making it a net 'negative feedback' loop. GPi and SNr: globus pallidus interna/substantia nigra, pars reticulata complex; GPe: globus pallidus external; SNc: substantia nigra, pars compacta; D1: dopamine D1-type receptor; D2: dopamine D2-type receptor; (+): excitatory projection; (−): inhibitory projection.

as injection of radiotoxic contrast agent. Thus, PWI, which uses quantitative rCBF measurements, has advantages in locating active brain regions, as well as increased capacity to detect abnormalities in brain function. Moreover, the time resolution of PWI is high enough to detect the activation of relative brain regions during symptom provocation, because the symptomatic state of OCD is maintained for a finite period of time once symptoms appear. In addition, PWI is a nonradiotoxic, relatively noninvasive imaging method that has been used widely and repeatedly to quantitatively analyze changes in cerebral hemodynamics occurring in a variety of mental disorders and brain illnesses. The latent toxicity of Gd-DTPA towards the kidneys was decreased by strictly controlling its dose by weight.

Our results, based on ROI-based image analysis, are mostly consistent with neurophysiological findings, suggesting that this post-processing of images is a feasible and reliable method to detect active brain regions during symptom provocation. The voxel-based statistical parametric mapping (SPM) method may fail to reflect inter-individual and interhemispheric morphological variabilities, since the method relies on the linear proportional scaling system of the Talairach atlas [22].

Certainly, the present study has some limitations. First, our arbitrarily defined ROIs may be too large to reflect functional units of brain activity. Therefore, significantly increased metabolic activity in some neuronal fields is likely to be obscured if surrounding areas within the same ROI show no changes or decreases in activity. MRI-based parceling of brain subregions may provide greater accuracy in standardizing ROIs across individuals [9,12]. Another limitation was that the current study had a relatively small sample size, and no male patients were included. Validation of our findings, therefore, requires larger numbers of patients and a comparison of various subgroups of patients with OCD. Lastly, it would be better that a non-OCD control group had been studied to make clear whether the changes of cerebral hemodynamics are associated with the general anxiety which triggered in patients by OCD-related fears or specific changes associated with the illness itself. It is a pity, however, that the findings obtained before our present study revealed that the significant increased ratings were not found while the non-OCD subjects were exposed to the aversive stimuli. Our present study focused on the changes of behavioral ratings and cerebral hemodynamics with the symptom provocation, while symptoms can not be significantly provoked by aversive stimuli in the non-OCD subjects. Up to the present, we have not found any relevant study which included a non-OCD control group.

In summary, we have shown that, during symptom provocation in OCD patients, abnormal features are particularly apparent in the orbitofrontal-subcortical circuits. The results obtained by PWI not only support the pathophysiological model of OCD, but also demonstrate the valuable application of PWI in revealing the brain structures involved in the pathophysiology of OCD.

## Acknowledgements

The authors thank Professor Song Lai, Yu-Feng Zang, and Xu-Chu Weng for helpful advice, and Professor Dong-Hong Gao for assistance in the data calculations and analyses.

## References

[1] M. Abbruzzese, S. Ferri, S. Scarone, The selective breakdown of frontal functions in patients with obsessive–compulsive disorder and in patients with schizophrenia: a double dissociation experimental finding, Neuropsychologia 35 (1997) 907–912.
[2] C.M. Adler, P. McDonough-Ryan, K.W. Sax, S.K. Holland, S. Amdt, S.M. Strakowski, fMRI of neuronal activation with symptom provocation in unmedicated patients with obsessive compulsive disorder, J. Psychiatr. Res. 34 (2000) 317–324.
[3] K. Alptekin, B. Degirmenci, B. Kivircik, H. Durak, B. Yemez, E. Derebek, Z. Tunca, Tc-99m HMPAO brain perfusion SPECT in drug-free obsessive–compulsive patients without depression, Psychiatry Res. 107 (2001) 51–56.
[4] L.R. Baxter Jr., J.M. Schwartz, K.S. Bergman, M.P. Szuba, B.H. Guze, J.C. Mazziotta, A. Alazraki, C.E. Selin, H.K. Ferng, P. Munford, M.E. Phelps, Caudate glucose metabolic rate changes with both drug and behavior therapy for obsessive–compulsive disorder, Arch. Gen. Psychiatry 49 (1992) 681–689.
[5] H.C. Breiter, S.L. Rauch, K.K. Kwong, J.R. Baker, R.M. Weisskoff, D.N. Kennedy, A.D. Kendrick, T.L. Davis, A. Jiang, M.S. Cohen, C.E. Stern, J.W. Belliveau, L. Baer, R.L. O' Sullivan, C.R. Savage, M.A. Jenike, B.R. Rosen, Functional magnetic resonance imaging of symptom provocation in obsessive–compulsive disorder, Arch. Gen. Psychiatry 53 (1996) 595–606.
[6] G.F. Busatto, C.A. Buchpiguel, D.R. Zamignani, G.E. Garrido, M.F. Glabus, M.C. Rosario-Campos, C.C. Castro, A. Maia, E.T. Rocha, P.K. McGuire, E.C. Miguel, Regional cerebral blood flow abnormalities in early-onset obsessive–compulsive disorder: an exploratory SPECT study, J. Am. Acad. Child Adolesc. Psychiatry 40 (2001) 347–354.
[7] L. Chang, T. Ernst, O. Speck, H. Patel, M. DeSilva, M. Leonido-Yee, E.N. Miller, Perfusion, MRI and computerized cognitive test abnormalities in abstinent methamphetamine users, Psychiatry Res. 114 (2002) 65–79.
[8] B. Crespo-Facorro, J.A. Cabranes, M.I. Lopez-Ibor Alcocer, B. Paya, C. Fernandez-Perez, M. Encinas, J.L. Ayuso-Mateos, J.J. Lopez-Ibor Jr., Regional cerebral blood flow in obsessive–compulsive patients with and without a chronic tic disorder: a SPECT study, Eur. Arch. Psychiatry Clin. Neurosci. 249 (1999) 156–161.
[9] B. Crespo-Facorro, J.J. Kim, N.C. Andreasen, R. Spinks, D.S. O'Leary, H.J. Bockholt, G. Harris, V.A. Magnotta, Cerebral cortex: a topographic segmentation method using magnetic resonance imaging, Psychiatry Res. 100 (2000) 97–126.
[10] A.R. Gilbert, G.J. Moore, M.S. Keshavan, L.A.D. Paulson, V. Narula, F.P. Mac-Master, C.M. Stewart, D.R. Rosenberg, Decrease in thalamic volumes of pediatric patients with obsessive–compulsive disorder who are taking paroxetine, Arch. Gen Psychiatry 57 (2000) 449–456.
[11] E. Hollander, I. Prohovnik, D.J. Stein, Increased cerebral blood flow during m-CPP exacerbation of obsessive–compulsive disorder, J. Neuropsychiatry Clin. Neurosci. 7 (1995) 485–490.
[12] J.J. Kim, B. Crespo-Facorro, N.C. Andreasen, D.S. O'Leary, B. Zhang, G. Harris, V.A. Magnotta, An MRI-based parcellation method for the temporal lobe, Neuroimage 11 (2000) 271–288.
[13] J.S. Kwon, J.J. Kim, D.W. Lee, J.S. Lee, D.S. Lee, M.S. Kim, I.K. Lyoo, M.J. Cho, M.C. Lee, Neural correlates of clinical symptoms

and cognitive dysfunctions in obsessive–compulsive disorder, Psychiatry Res. 122 (2003) 37–47.
[14] P.K. McGuire, C.J. Bench, C.D. Frith, L.M. Marks, R.S. Frackowiak, R.J. Dolan, Functional anatomy of obsessive–compulsive phenomena, Br. J. Psychiatry 164 (1994) 459–468.
[15] D. Perani, C. Colombo, S. Bressi, A. Bonfanti, F. Grassi, S. Scarone, L. Bellodi, E. Smeraldi, F. Fazio, [18F]FDG-PET study in obsessive–compulsive disorder: a clinical metabolic correlation study after treatment, Br. J. Psychiatry 166 (1995) 244–250.
[16] S.L. Rauch, M.A. Jenike, N.M. Alpert, L. Baer, H.C. Breiter, C.R. Savage, A.J. Fischman, Regional cerebral blood flow measured during symptom provocation in obsessive–compulsive disorder using oxygen 15-labeled carbon dioxide and positron emission tomography, Arch. Gen. Psychiatry 51 (1994) 62–70.
[17] R.T. Rubin, J. Villanueva-Meyer, J. Ananth, P.G. Trajmar, I. Mena, Regional xenon-133 cerebral blood flow and cerebral technetium 99m-HMPAO uptake in unmedicated patients with obsessive–compulsive disorder and matched normal control patients: determination by high-resolution single-photon emission computed tomography, Arch. Gen. Psychiatry 49 (1992) 695–702.
[18] R.H. Saric, T.E. Schlaepfer, B.D. Greenberg, D.R. McLeod, G.D. Pearlson, S.H. Wong, Cerebral blood flow in obsessive–compulsive patients with major depression: effect of treatment with sertraline or desipramine on treatment responders and non-responders, Psychiatry Res. 108 (2001) 89–100.
[19] S. Saxena, A.L. Brody, K.M. Maidment, J.J. Dunkin, M. Colgan, S. Alborzian, M.E. Phelps, L.R. Baxter Jr., Localized orbitofrontal and subcortical metabolic changes and predictors of response to paroxetine treatment in obsessive–compulsive disorder, Neuropsychophamacology 21 (1999) 683–693.
[20] S. Saxena, A.L. Brody, J.M. Schwartz, L.R. Baxter, Neuroimaging and frontal-subcortical circuitry in obsessive–compulsive disorder, Br. J. Psychiatry Suppl. 35 (1998) 26–37.
[21] S.E. Swedo, P. Pietrini, H.L. Leonard, M.B. Schapiro, D.C. Rettew, E.L. Goldberger, J.L. Rapoport, C.L. Grady, Cerebral glucose metabolism in childhood-onset obsessive–compulsive disorder, Arch. Gen. Psychiatry 49 (1992) 690–694.
[22] J. Talairach, P. Tournoux, Co-Planar Stereotaxic Atlas of the Human Brain, Thieme Medical Publishers Inc., New York, 1988.